



Serial No. N6790

NAFO SCR Doc. 18/007

**SCIENTIFIC COUNCIL MEETING – JUNE 2018****Biological Oceanographic Conditions in the Northwest Atlantic During 2017**

by

D. Bélanger<sup>1</sup>, G. Maillet<sup>1</sup>, P. Pepin<sup>1</sup>, B. Casault<sup>2</sup>, C. Johnson<sup>2</sup>, S. Plourde<sup>3</sup>, P.S. Galbraith<sup>3</sup>, L. Devine<sup>3</sup>, M. Scarratt<sup>3</sup>, M. Blais<sup>3</sup>, E. Head<sup>2</sup>, C. Caverhill<sup>2</sup>, E. Devred<sup>2</sup>, J. Spry<sup>2</sup>, A. Cogswell<sup>2</sup>, L. St-Amand<sup>3</sup>, S. Fraser<sup>1</sup>, G. Doyle<sup>1</sup>, A. Robar<sup>1</sup>, J. Hingdon<sup>1</sup>, J. Holden<sup>1</sup>, C. Porter<sup>2</sup>, E. Colbourne<sup>1</sup>

**Abstract**

Biological and chemical variables collected in 2017 from coastal high frequency monitoring stations, semi-annual oceanographic sections, and ships of opportunity ranging from the Labrador-Newfoundland and Grand Banks Shelf (Subareas 2 and 3), extending west into the Gulf of St. Lawrence (Subarea 4) and further south along the Scotian Shelf and the Bay of Fundy (Subarea 4) and into the Gulf of Maine (Subarea 5) are presented and referenced to previous information from earlier periods when available. We review the interannual variations in inventories of nitrate, chlorophyll *a* and indices of the spring bloom inferred from satellite ocean colour imagery, as well as the abundance of major functional taxa of zooplankton collected as part of the 2017 Atlantic Zone Monitoring Program (AZMP). All time series are presented in terms of anomalies relative to a 1999-2015 climatology. In general, 2017 nitrate inventories in the upper (0-50m) water column were near normal throughout the Northwest Atlantic with the exception of higher positive anomalies on the southeastern Grand Banks (3LNO) and the western Scotian Shelf (4Vs), and negative anomaly at the high frequency sampling station Prince 5 in the Bay of Fundy (4X). The deeper (50-150m) nitrate inventories remained mostly near to below normal on the Newfoundland and Labrador Shelves and on the Grand Banks. The depleted inventories of deep nitrate observed on most of the Scotian shelf in 2015 continued to decline in all subregions (4VWX) in 2017. The chlorophyll *a* inventories inferred from the seasonal AZMP oceanographic surveys and high frequency sampling stations were above normal in the Gulf of St. Lawrence and below normal on the southeastern Grand Banks (including Flemish Cap) and the Scotian Shelf in 2017. Variation in shallow and deep composite indices of nitrate concentration and chlorophyll *a* biomass showed similar trends during the 1999-2017 time series suggesting regulation of phytoplankton production through nitrate availability throughout the zone. The spring bloom magnitude and amplitude in 2017 continued below climatology in virtually all statistical subregions on the Canadian continental Shelves and in the Gulf of St. Lawrence, and above or near normal in the Labrador Sea. Spring bloom peak timing occurred later than normal in the Labrador Sea and on the NL and the Scotian shelves and varied in the Gulf of St. Lawrence, whereas bloom duration stayed near normal throughout the study area except for a markedly longer bloom in the NW Gulf of St. Lawrence. The abundance of the small copepod *Pseudocalanus* spp. remained high on the NL Shelf but declined in the Gulf of St. Lawrence and on the Scotian Shelf, while the abundance of the large copepod *Calanus finmarchicus* stayed below normal in most NAFO Subareas from northern Labrador (2J) to the western Scotian Shelf (4X). Despite the generally near to above normal abundance of total copepods and the high abundance of non-copepods throughout the study area in 2017, total zooplankton biomass stayed unusually low for a third year in a row. Finally, significant correlations between climate, ocean chemistry and phytoplankton and zooplankton standing stocks anomaly time series were observed at both zonal (Northwest Atlantic) and regional (NL Shelf) scale.



## 1. Introduction

We review biological and chemical oceanographic conditions on the Newfoundland and Labrador (NL) Shelf, Grand Bank (GB), Gulf of St. Lawrence (GSL), Scotian Shelf (SS), and Gulf of Maine during 2017, and reference earlier periods where data are available. Directed sampling from research vessels on oceanographic sections and ships of opportunity at coastal high frequency sampling stations by the Atlantic Zone Monitoring Program (AZMP<sup>1</sup>) and the completion of seasonal oceanographic surveys during 2017 provided reasonable spatial and temporal series coverage but some gaps occurred as a result of vessel availability. Collection of standard variables (temperature, salinity, nutrients, chlorophyll, zooplankton abundance and composition) affords a foundation for comparison with previous years. Additional details regarding physical, biological and chemical oceanographic conditions in the Northwest (NW) Atlantic in 2016 and earlier years can be found in Colbourne *et al.* (2015, 2016), Devine *et al.* (2015, 2017), and DFO (2015), Galbraith *et al.* (2015, 2016), Hebert *et al.* (2015, 2016, 2018), Johnson *et al.* (2016, 2017, 2018), Pepin *et al.* (2015, 2017), Plourde *et al.* (2014), Yashayaev *et al.* (2014).

## 2. Methods

Collections of standard AZMP variables are based on sampling protocols outlined by Mitchell *et al.* (2002). Observations for 2017 and earlier years presented in this document are based on seasonal surveys conducted during the spring through the autumn (typically March through December). The coastal high frequency sampling stations are typically sampled at twice monthly to monthly intervals during ice-free conditions. The location of the standard oceanographic sections and coastal high frequency sampling stations are shown in Figure 1.

Phytoplankton biomass was estimated from ocean colour data collected by the Sea-viewing Wide Field-of-view Sensor (SeaWiFS; <http://seawifs.gsfc.nasa.gov/SEAWIFS.html>), Moderate Resolution Imaging Spectroradiometer (MODIS) “Aqua” sensor (<http://modis.gsfc.nasa.gov/>), and the Visible-Infrared Imager Radiometer Suite (VIIRS) sensor (<https://oceancolor.gsfc.nasa.gov/data/viirs-snpp/>). The SeaWiFS time series began in the September of 1997, MODIS data stream began in July, 2002, and VIIRS availability is January 2012 to present. Satellite data do not provide information on the vertical structure of chlorophyll *a* (chl *a*) in the water column but do provide highly resolved (~1.5 km) data on their geographical distribution in surface waters at the large scale. Composite images of 8-days for chl *a* for the entire NW Atlantic (39-62.5° N Latitude 42-71° W Longitude) were routinely produced from SeaWiFS/MODIS/VIIRS data<sup>2</sup>. Basic statistics (mean, range, standard deviation, etc.) were extracted from the composites for selected statistical subregions as shown in Figure 1. Ocean colour time series from 1998 to 2017 were constructed using data from the available satellite sensors using the following periods: 1998-2007 SeaWiFS, 2008-2011 MODIS, and 2012-2017 VIIRS.

Standardized annual anomalies were developed as a method of summarizing the many variables used to represent the state of lower trophic levels. To simplify the information, the time series of the annual estimate of inventory or abundance for each variable was standardized to a mean of zero (for the period 1998-2015 for ocean colour data, and 1999-2015 for AZMP surveys) and unit standard deviation ( $[\text{observation} - \text{mean}]/\text{SD}$ ). The standard deviation (SD) provides a measure of the variability of an index. The result of this standardization yields a series of annual anomalies. The anomalies serve to illustrate departures from the long-term mean across the range of variables. Values near the mean (e.g. 0 anomaly) indicate near normal, positive values indicate above/late trends compared to the climatology, and negative values indicate below/earlier trends. The difference between a given year and the climatological mean represents the magnitude of that departure from the long-term climatology. To capture longer-term trends in the chemical-biological observations throughout the studied area, a cumulative (or composite) anomaly index was calculated for each sampling year by summing the annual anomalies of each NAFO Subareas. In 2017, the reference period was extended to 1998/1999-2015, compared to 1998/1999-2010 for previous reports. Considering the non-stationary state of the Atlantic system, extending the climatology to include recent years changes the mean against which observations are compared, which can shift the sign or magnitude of anomalies. While this issue must be kept

<sup>1</sup> <http://www.meds-sdmm.dfo-mpo.gc.ca/isdm-gdsi/azmp-pmza/index-eng.html>

<sup>2</sup> <http://www.bio.gc.ca/science/newtech-technouvelles/sensing-teledetection/index-en.php>

in mind, the advantage of the extended reference period is to provide more relevant depictions of current system conditions and trends and place the observations in context with past levels of variability. Moreover, extending the reference period does not alter the general anomaly patterns for the time series. For the chemical-biological observations, the key variables selected were: (1) near surface (0-50 m) and deep (50-150 m) nitrate inventories, and (2) 0-100m integrated chl *a*, satellite indices of the magnitude, amplitude, peak timing and duration of the spring bloom (Zhai *et al.* 2011), and zooplankton abundance for different functional zooplankton taxa (*Pseudocalanus* spp., *Calanus finmarchicus*, total copepods, and total non-copepods).

### 3. Annual Variability in Nutrient, Phytoplankton, and Zooplankton Conditions in the NAFO Subareas

#### 3.1 Nitrate and Chlorophyll *a*

The shallow (0-50 m) nitrate inventories for 2017 were near the climatological mean throughout the NW Atlantic with the exception of larger positive and negative anomalies for the SE Grand Banks section (3LNO) and the Prince 5 high frequency sampling station (Bay of Fundy, 4X), respectively. This represents a general increase from 2016 especially on the GB, the GSL and the SS where Anomalies were mostly negative (Figure 2A). The deep (50-150 m) nitrate inventories were near or below climatology across the NW Atlantic with markedly low concentrations observed on the SS (4VWX). This represents a decrease in deep nitrate inventories for most of NAFO Subarea compared to 2016 (Figure 2B). In general, composite anomalies in shallow nitrate inventories were mostly near or above normal during the first half of the time series, before starting to decline in 2008 to a record-low in 2010. Shallow inventories subsequently increased steadily from 2010 to 2015 and declined again in 2016 to the second lowest values of the time-series. In 2017 shallow nitrate inventories were back to near normal values (Figure 3A). The corresponding time series for deep nitrate inventories generally followed the pattern of variation observed in the upper water column except for 2017 where inventories continued to decline and reached a time series record-low (Figure 3B).

The chlorophyll (Chl) *a* inventories inferred from the seasonal oceanographic surveys, which provides an index of phytoplankton biomass throughout the water column, were generally near normal (anomalies within 1 SD) across the NW Atlantic. Anomalies were negative on the Flemish Cap and the GB (3LMNO) as well as on the SS (3P4VW), and positive in the GSL (4RST). The general spatial pattern of variation in Chl *a* concentrations is similar to 2016 with marked increases for the Flemish Cap and the southern GSL (Figure 4). The composite anomaly time series showed an overall negative trend from the start of the series until a record-low observed in 2011, punctuated by a brief record-high in 2007. Since 2010, Chl *a* biomass remained near or below climatology (Figure 5A). Trends in composite anomalies for both shallow and deep nitrate inventories generally tracked each other, as well as the trend in chlorophyll biomass, across Subareas 2-4 (Figure 5B).

#### 3.2 Phytoplankton Spring Bloom

The magnitude of the spring phytoplankton bloom (total phytoplankton production) was either near or below normal across all subregions except for one exceptionally large bloom observed at the Bravo sub-region in the Labrador Sea (Figure 6). The amplitude (peak intensity) of the spring bloom was consistently below normal throughout Subareas 0B to 5 with positive anomalies only observed on the Greenland Shelf and in the Labrador Sea (Figure 7). These trends are consistent with the observations from 2016 where both spring bloom magnitude and amplitude were below the climatological average across the study area, with exceptions in the Labrador Sea and in the Cabot Strait (magnitude), and in the GSL (amplitude) (Figure 6 & 7).

Spring bloom peak production timing varied throughout the NW Atlantic but stayed near the climatological average (~ 1 SD) in most subregions. Later blooms (positive anomalies) were observed for the Labrador Sea (1F2GH), the Newfoundland Shelf and the GB (including the Flemish Cap) (3KLMNOPs), the SS (4VWX), and the Georges Bank (5Ze), while early blooms (negative anomalies) were observed on the Greenland Shelf (1F), the Labrador Shelf (2HJ), in the northeast GSL (4RS), and in the Cabot Strait (4Vs). In general, the spring bloom in the GSL and on the SS and the Georges Bank occurred later in 2017, compared to the previous year (Figure 8). The duration of the spring bloom was near the climatological average across all NW Atlantic subregions except for the northwest GSL where a longer bloom (positive anomaly) was observed. The exceptionally long bloom observed in 2016 for the Flemish Cap, the Cabot Strait and the western SS were back to normal values in 2017 (Figure 9).

Time series of composite standardized anomalies were constructed for each ocean colour index extending back to the start of SeaWiFS in 1998. Overall, the magnitude of the spring bloom showed small changes from 1998 until 2005 followed by an increasing trend from 2006 until a record-high in 2011 and a subsequent decline through 2017 (Figure 10A). Changes in the amplitude of the spring bloom closely followed the trends observed in magnitude with limited change through 2005 followed by an increasing trend with a record-high in 2011, and by a decline to a time series record low in 2017 (Figure 10B). Peak timing of the spring bloom shifted between periods of early-late blooms throughout the 20-year time series and have stayed above normal (late blooms) since 2013 (Figure 11A). A gradual reduction in the duration of the spring bloom was observed from the late 1990's to 2011 across the subregions before stabilizing below normal until 2015. Duration reached a record high in 2016 as a result of some exceptional long-duration blooms observed throughout the zone ranging from the Hudson Strait in 0B to Subarea 5 in the GoM (Figure 9), and was back to near normal in 2017 (Figure 11B).

### 3.3 Zooplankton Abundance and Biomass

*Pseudocalanus* spp. is a dominant small epipelagic copepod and an important preferred prey for many early life stages of fish. In 2017, *Pseudocalanus* spp. abundances were near to above normal on the NL Shelf and the GB (2J3KLN0) and below to near normal on the SS and in the GSL except at the Rimouski high frequency sampling station where a high positive anomaly was recorded. A general decline in *Pseudocalanus* spp. abundance was observed in the entire GSL in 2017 compare to the previous year (Figure 12A). The abundance of the large grazing copepod, *Calanus finmarchicus*, another dominant species and important prey item to higher trophic levels, remained below or near normal across the entire survey area in 2017. Observations from 2016 and 2017 showed similar spatial pattern of *C. finmarchicus* abundance throughout the study area (Figure 12B). The abundance of all combined copepod taxa varied across the NW Atlantic in 2017. Copepod abundances were generally within 1 SD from climatology, with larger positive and negative anomalies observed for the SE Grand Banks section (3LNO) and at the Rimouski high frequency sampling station (4T), respectively. This represents a general decline in copepod abundance from the previous year when abundances were either near or above normal across the entire survey area, with a markedly large positive anomaly for the Rimouski high frequency sampling station (Figure 13A). The non-copepod taxa (mostly larval stages of benthic invertebrates, gelatinous and carnivorous zooplankton) remained above normal throughout most of the study area in 2017. The spatial anomaly pattern in 2017 was similar to 2016, with the exception of sharp decreases in the northern GSL (4RS) and on the eastern SS (4Vs) (Figure 13B).

Composite anomaly time series were constructed for each of the functional zooplankton groups extending back to the initiation of the monitoring program in 1999. The abundance anomaly time series for the small grazing copepod *Pseudocalanus* spp. was relatively stable with no distinct trend from 1999-2011. Abundance then declined to a record low in 2012 before rapidly increasing to a record high in 2015. Abundance was back to below normal in 2017 after a marked decline in *Pseudocalanus* abundance in the GSL (Figure 14A). The *C. finmarchicus* anomaly time series showed a positive trend from the beginning of the monitoring program to a record-high in 2006 followed by a general decline to a record-low in 2015. Abundances have remained low over the past couple years with the third and second lowest anomalies of the time series recorded in 2016 and 2017, respectively (figure 14B). Total copepod abundance oscillated around the climatological average over the entire time series. A strong increasing trend was noted from 2013 to a peak in 2016, with positive anomalies in nearly all NAFO subareas, followed by a decline to near normal value in 2017 (Figure 15A). Non-copepod abundance stayed relatively stable during the first half of the time series before starting to steadily increase to a record-high in 2016 with positive anomalies in all subareas across the NW Atlantic. Despite a decline relative to 2016, abundances stayed above normal in 2017 with negative anomalies only observed in few subareas (Figure 15B). Zooplankton biomass increased from the beginning of the time series to a record high in 2003, followed by a general declining trend until 2012-2014. This was followed by an abrupt decrease in biomass to a record low in 2015 after which biomass has remained well below the climatological average throughout the NW Atlantic (Figure 16).

#### 4. Ocean Climate, Nutrients and Primary Production Indices

Pearson correlations were used to investigate relationships among composite anomaly time series for the chemical (nitrate) and biological (Chl *a*, satellite ocean colour, and zooplankton abundance) indices throughout the NW Atlantic (zonal scale) and on the NL Shelf (regional scale) (Figure 18 & 19). At a regional scale, a composite climate index derived from a variety of meteorological, sea ice, ocean temperature, and salinity time series across NAFO Divisions 2-4 (Colbourne et al., 2017) was used to examine potential links between the physical environment and chemical-biological observations (Figure 17). Nitrate concentration in the upper portion of the water column is a good indicator of the ongoing phytoplankton production, whereas nitrate concentration in the deeper layer of the ocean is normally related to the primary production of the following year, when deep nitrate becomes available to primary producers after being transported near the surface by vertical mixing. Chl *a* anomalies were correlated to shallow nitrate ( $p=0.03$ ,  $r^2=0.24$ ) at the zonal scale, and to deep nitrate ( $p=0.02$ ,  $r^2=0.31$ ) at the regional scale. On the NL Shelf, spring bloom magnitude ( $p<0.01$ ,  $r^2=0.45$ ), amplitude ( $p=0.02$ ,  $r^2=0.27$ ) and peak timing ( $p<0.01$ ,  $r^2=0.56$ ) were correlated with the composite climate index and showed an association between warmer climatic conditions and early, important spring blooms, highlighting the potential cascading effects of climate on regional oceanic productivity. The negative correlation between spring bloom peak timing and magnitude observed both regionally ( $p=0.03$ ,  $r^2=0.25$ ) and zonally ( $p=0.03$ ,  $r^2=0.25$ ) likely reflected similar trade-offs across the NW Atlantic between phytoplankton production and zooplankton grazing, i.e., mismatch between early bloom and zooplankton propagation allows phytoplankton biomass to further develop. Regional climatic index was positively correlated ( $p<0.01$ ,  $r^2=0.38$ ) with *C. finmarchicus* abundance and negatively correlated ( $p<0.01$ ,  $r^2=0.38$ ) with *Pseudocalanus* spp. abundance indicating higher *C. finmarchicus* abundance during warmer period and higher *Pseudocalanus* abundance during colder climatic episodes. Moreover, high *Pseudocalanus* spp. abundances were associated with later spring blooms (positive correlation with peak timing) both regionally ( $p=0.01$ ,  $r^2=0.39$ ) and zonally ( $p=0.02$ ,  $r^2=0.30$ ). These correlations suggest that climatic conditions and bottom up forcing play a role in controlling copepod community structure. Finally, observed differences between zonal and regional correlations reflected the importance of regional scale linkages between climatic conditions, the chemical environment, and ocean productivity in interpreting and forecasting oceanographic processes relevant to stock assessment.

#### 5. Biological Oceanographic Highlights in 2017

- Nitrate inventories in the upper (0-50m) water-column were near normal compared to the 1999-2015 climatology throughout the NW Atlantic with the exception of larger positive and negative anomalies on the SE Grand Banks section (3LNO) and at station Prince 5 in the Bay of Fundy (4X), respectively.
- The deeper (50-150m) nitrate inventories were near normal throughout the surveyed area except on the SS (3P, 4VWX) where deep nitrate concentrations continued below normal.
- The chlorophyll *a* inventories inferred from the seasonal AZMP oceanographic surveys and fixed stations were below normal on the GB (3LNMO) and the eastern SS (4VW), above normal in the southern GSL (4T), and near normal in the other Subareas.
- Chl *a* biomass was positively correlated with shallow nitrate concentrations at zonal scale (NW Atlantic), and positively correlated with 1-y lag deep nitrate concentrations at the regional scale (Newfoundland and Labrador) suggesting regulation of phytoplankton production through nitrate availability across Subareas 2-4.
- Both the magnitude and amplitude metrics of the spring bloom were mostly below the long-term climatology over the 25 statistical subregions.
- Spring bloom peak timing was later than normal throughout most of the NW Atlantic with the exception of the Greenland (1F2GH) and the northern Labrador (2HJ) shelves, the northern GSL (4RS) and the Cabot Strait (3Pn4Vn) where early blooms were observed.
- Zooplankton abundances (both copepods and non-copepods) showed a general decline in 2017 across the AZMP standard sections and high frequency sampling stations.
- Zooplankton biomass remained below normal across the surveyed area in 2017 with the third consecutive lowest composite anomaly of the time series.

- Abundance of *Pseudocalanus* spp. reflected the general pattern of change in small copepod abundance, whereas abundance of the larger copepod *Calanus finmarchicus* reflected the general pattern of change in total zooplankton biomass.
- Differences between zonal (NW Atlantic) and regional (Newfoundland and Labrador) correlations reflected the importance of regional scale linkages between climatic conditions, the chemical environment and ocean production at lower trophic levels.

## Acknowledgements

We thank the staff at Fisheries and Oceans Canada's Northwest Atlantic Fisheries Centre (NAFAC) Biological and Physical Oceanography Section, Bedford Institute of Oceanography (BIO), Ocean and Ecosystem Sciences Division (OESD), and the Institute Maurice Lamontagne (IML), Pelagic and Ecosystem Science Branch, for their acquisition, quality control and archiving of the data. We also wish to thank the efforts of the many Scientific Assistants and Science Staff at the Northwest Atlantic Fisheries Centre in St. John's, the Bedford Institute of Oceanography, the Institute Maurice Lamontagne, and the St. Andrews Biological Station and CCGS Teleost, CCGS Needler, and CCGS Hudson Officers and Crew for their invaluable assistance at sea. The expertise of Jackie Spry was crucial to the completion of this work.

## References

- Colbourne, E., Holden, J., Senciall, D., Bailey, W., Craig, J. and S. Snook. 2015. Physical Oceanographic Conditions on the Newfoundland and Labrador Shelf during 2014. DFO Can. Sci. Advis. Sec. Res. Doc. 2015/053. v+ 37 p.
- Colbourne, E., Holden, J., Senciall, D., Bailey, W., S. Snook and J. Higdon. 2016. Physical Oceanographic Conditions on the Newfoundland and Labrador Shelf during 2015. DFO Can. Sci. Advis. Sec. Res. Doc. 2016/079. v +40 p.
- Colbourne, E., Holden, J., Snook, S., Han, G. Lewis, S., Senciall, D., Bailey, W., Higdon, J. and Chen, N. 2017. Physical Oceanographic Conditions on the Newfoundland and Labrador Shelf during 2016. DFO Can. Sci. Advis. Sec. Res. Doc. 2017/079. v + 50 p.
- Devine, L., Plourde, S., Starr, M., St-Pierre, J.-F., St-Amand, L., Joly, P. and Galbraith, P. S. 2015. Chemical and Biological Oceanographic Conditions in the Estuary and Gulf of St. Lawrence during 2013. DFO Can. Sci. Advis. Sec. Res. Doc. 2015/013. v + 45 pp.
- Devine, L., Scarratt, M., Plourde, S., Galbraith, P.S., Michaud, S. and Lehoux, C. 2017. Chemical and Biological Oceanographic Conditions in the Estuary and Gulf of St. Lawrence during 2015. DFO Can. Sci. Advis. Sec. Res. Doc. 2017/034. v + 48 p.
- DFO. 2015. Oceanographic conditions in the Atlantic zone in 2014. DFO Can. Sci. Advis. Sec. Sci. Advis. Rep. 2015/030
- Galbraith, P.S., Chassé, J., Nicot, P., Caverhill, C., Gilbert, D., Pettigrew, B., Lefaiivre, D., Brickman, D., Devine, L., and Lafleur, C. 2015. Physical Oceanographic Conditions in the Gulf of St. Lawrence in 2014. DFO Can. Sci. Advis. Sec. Res. Doc. 2015/032. v + 82 p.
- Galbraith, P.S., Chassé, J., Caverhill, C., Nicot, P., Gilbert, D., Pettigrew, B., Lefaiivre, D., Brickman, D., Devine, L., and Lafleur, C. 2016. Physical Oceanographic Conditions in the Gulf of St. Lawrence in 2015. DFO Can. Sci. Advis. Sec. Res. Doc. 2016/056. v + 90 p.
- Galbraith, P.S., Chassé, J., Caverhill, C., Nicot, P., Gilbert, D., Pettigrew, B., Lefaiivre, D., Brickman, D., Devine, L., and Lafleur, C. 2016. Physical Oceanographic Conditions in the Gulf of St. Lawrence in 2015. DFO Can. Sci. Advis. Sec. Res. Doc. 2017/044. v + 91 p.
- Head, J.H.E., Pepin, P. 2010. Spatial and inter-decadal variability in plankton abundance and composition in the Northwest Atlantic (1958–2006). *J. Plank. Res.* 32(12): 1633-1648 pp.

### References (continued)

- Hebert, D., Pettipas, R., Brickman, D., and Dever, M. 2015. Meteorological, Sea Ice and Physical Oceanographic Conditions on the Scotian Shelf and in the Gulf of Maine during 2014. DFO Can. Sci. Advis. Sec. Res. Doc. 2015/040. v + 49 p.
- Hebert, D., Pettipas, R., Brickman, D., and Dever, M. 2016. Meteorological, sea ice and physical oceanographic conditions on the Scotian Shelf and in the Gulf of Maine during 2015. DFO Can. Sci. Advis. Sec. Res. Doc. 2016/083. v + 49 p.
- Hebert, D., Pettipas, R., Brickman, D., and Dever, M. 2018. Meteorological, Sea Ice and Physical Oceanographic Conditions on the Scotian Shelf and in the Gulf of Maine during 2016. DFO Can. Sci. Advis. Sec. Res. Doc. 2018/016. v + 53 p.
- Johnson, C., Casault, B., Head, E., and Spry, J. 2016. Optical, Chemical, and Biological Oceanographic Conditions on the Scotian Shelf and in the Eastern Gulf of Maine in 2014. DFO Can. Sci. Advis. Sec. Res. Doc. 2016/003. v + 51 p.
- Johnson, C., Pepin, P., Curtis, K.A., Lazin, G., Casault, B., Colbourne, E., Galbraith, P.S., Harvey, M., Herbert, D., Maillet, G., and Starr, M. 2014. Indicators of Pelagic Habitat Status in the Northwest Atlantic. DFO Can. Sci. Advis. Sec. Res. Doc. 2014/047. v + 74 p.
- Johnson, C., Devred, E., Casault, B., Head, E., and Spry, J. 2017. Optical, Chemical, and Biological Oceanographic Conditions on the Scotian Shelf and in the Eastern Gulf of Maine in 2015. DFO Can. Sci. Advis. Sec. Res. Doc. 2017/012. v + 53 p.
- Johnson, C., Devred, E., Casault, B., Head, E., and Spry, J. 2018. Optical, Chemical, and Biological Oceanographic Conditions on the Scotian Shelf and in the Eastern Gulf of Maine in 2016. DFO Can. Sci. Advis. Sec. Res. Doc. 2018/017. v + 58 p.
- Mitchell, M.R., Harrison, G., Pauley, K., Gagné, A., Maillet, G., Strain, P. 2002. Atlantic Zone Monitoring Program Sampling Protocol. Canadian Technical Report of Hydrography and Ocean Sciences 223, 23 pp.
- Pepin, P., Maillet, G., Fraser, S., Shears, T. and Redmond G. 2015. Optical, chemical, and biological oceanographic conditions on the Newfoundland and Labrador Shelf during 2013. DFO Can. Sci. Advis. Sec. Res. Doc. 2015/027. v + 37p.
- Pepin, P., Maillet, G., Fraser, S., Doyle, G., Robar, A., Shears, T., and Redmond, G. 2017 Optical, chemical, and biological oceanographic conditions on the Newfoundland and Labrador Shelf during 2014-2015. DFO Can. Sci. Advis. Sec. Res. Doc. 2017/009. v + 37 p.
- S. Plourde, Starr, M., Devine, L., St-Pierre, J.-F., St-Amand, L., Joly, P., and Galbraith, P. S. 2014. Chemical and biological oceanographic conditions in the Estuary and Gulf of St. Lawrence during 2011 and 2012. DFO Can. Sci. Advis. Sec. Res. Doc. 2014/049. v + 46 pp
- Yashayaev, I., Head, E.J.H., Azetsu-Scott, K., Ringuette, M., Wang, Z., Anning, J., and Punshon, S. 2014. Environmental Conditions in the Labrador Sea during 2013. DFO Can. Sci. Advis. Sec. Res. Doc. 2014/105. v +35 p.
- Zhai, L., Platt, T., Tang, C., Sathyendranath, S., and Hernández Walls, R. 2011. Phytoplankton phenology on the Scotian Shelf. – ICES Journal of Marine Science, 68: 781–791.

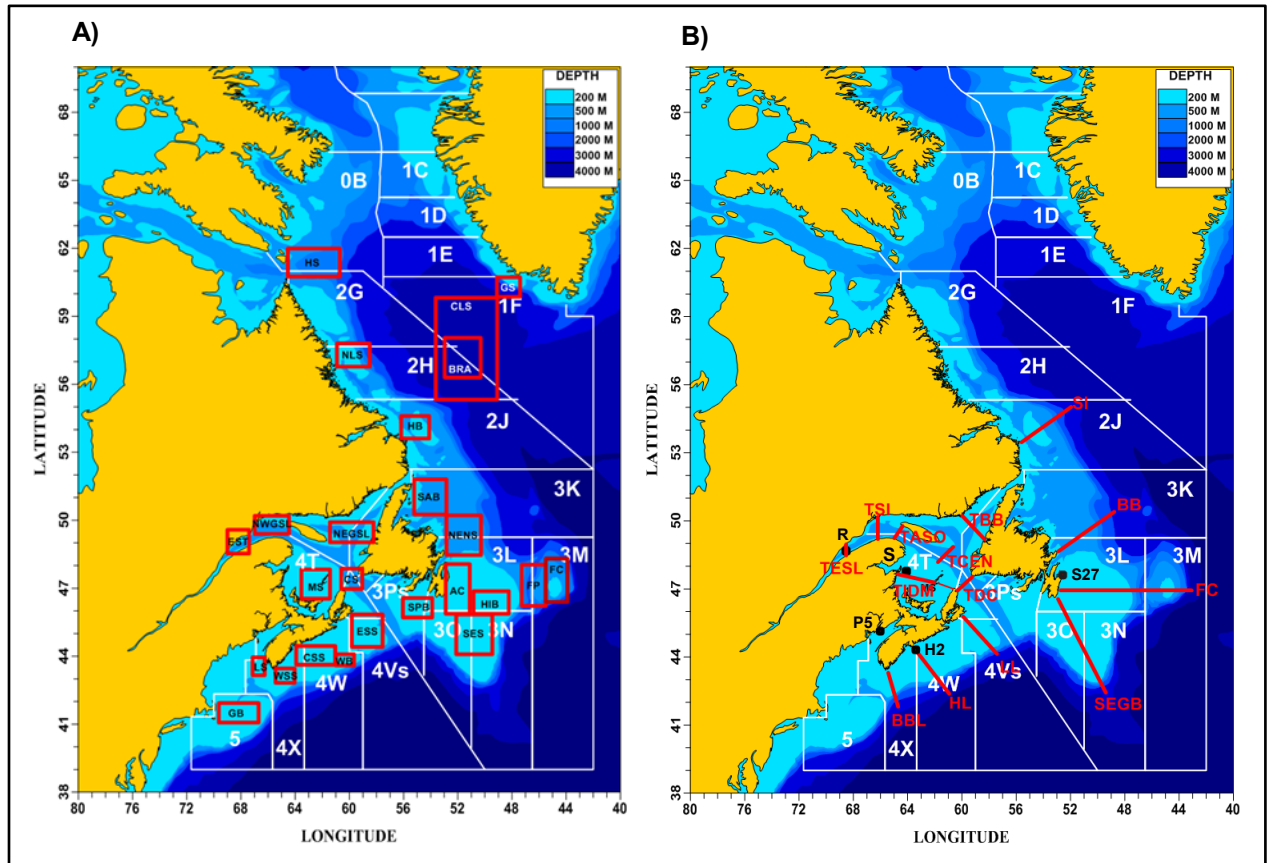


**Fig. 1** (A) Location of the statistical subregions from which satellite Ocean colour metrics (magnitude, amplitude, peak timing and duration of spring bloom) were derived (HS=Hudson Strait, GS=Greenland Shelf, CLS=central Labrador Sea, BRA=ocean station Bravo, NLS=northern Labrador Shelf, LS=Labrador Shelf, HB=Hamilton Bank (Seal Island), SAB=St. Anthony Basin, NENS=northeast Newfoundland Shelf, AC=Avalon Channel, FP=Flemish Pass, FC=Flemish Cap, HIB=Hibernia, SPB=St. Pierre Bank, SES=southeast Shoal, CS=Cabot Strait, MS=Magdalen Shallows, NEGSL=northeast Gulf of St. Lawrence, NWGSL=northwest Gulf of St. Lawrence, EST = Estuary, ESS=eastern Scotian Shelf, WB=Western Bank, CSS=central Scotian Shelf, WSS=western Scotian Shelf, LS=Lurcher Shoal, GB=Georges Bank. (B) Location of primary Atlantic Zone Monitoring Program (AZMP) sections (red lines: SI=Seal Island, BB=Bonavista Bay, FC=Flemish Cap, SEG=Southeastern Grand Banks, TBB and TCEN=northeast Gulf of St. Lawrence, TESL, TSI and TASO=northwest Gulf of St. Lawrence, TIDM=southern Gulf of St. Lawrence, TDC=Cabot Strait, LL=Louisbourg Line, HL=Halifax Line, BBL=Brown Bank Line), and coastal high frequency sampling stations (black squares: S27=Station 27, R=Rimouski, S=Shediac, H2=Halifax-2, P5=Prince-5) from which chemical (nitrate) and biological (chlorophyll *a* and zooplankton) data were collected.

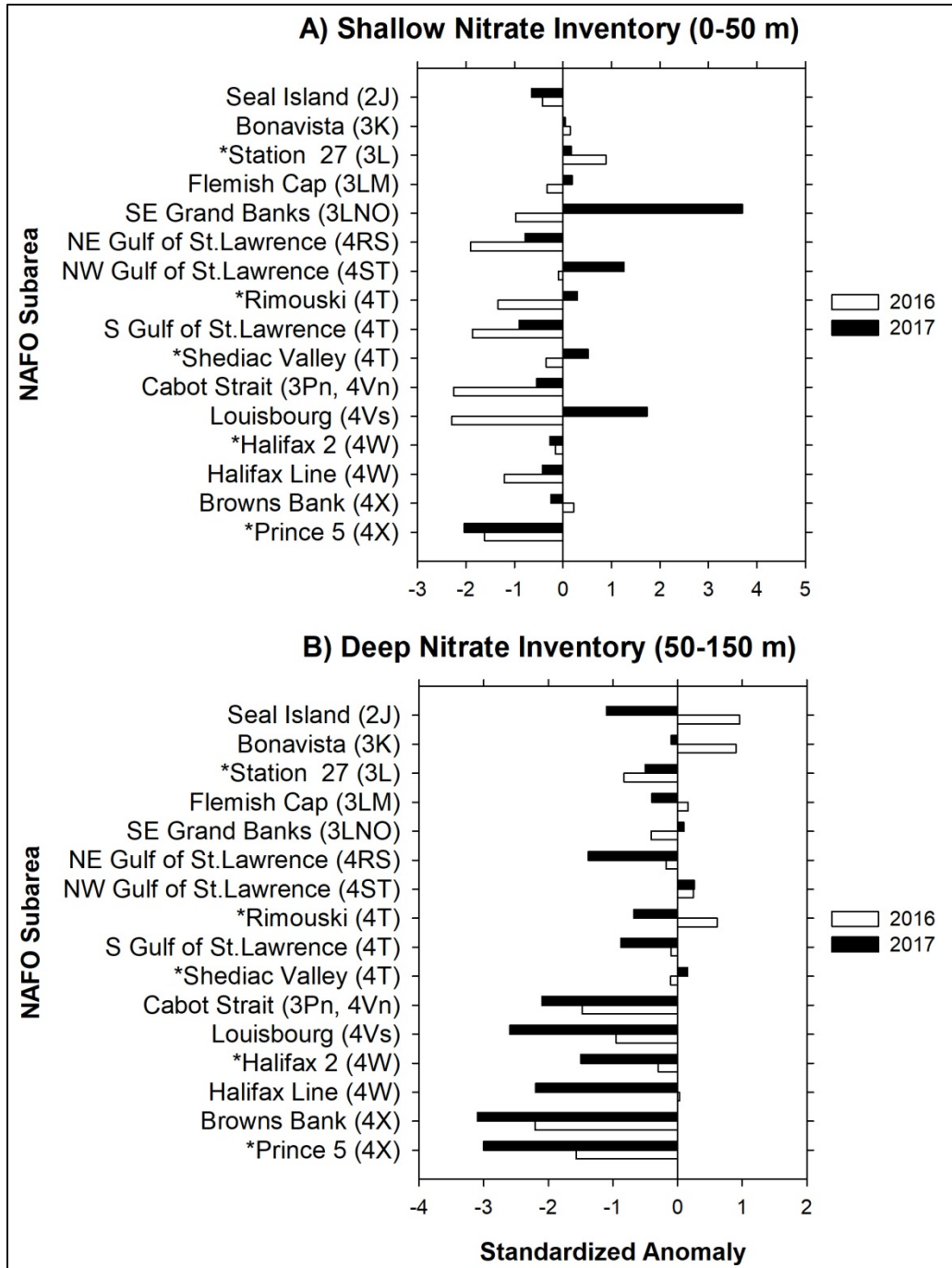


**Fig. 2** Summary of nitrate (combined nitrate and nitrite) inventories for (A) the upper (0-50m) water column, and (B) the lower (50-150m) water column from different oceanographic sections and high frequency sampling stations during the 2016 and 2017 AZMP surveys. The standardized anomalies are the differences between the annual mean for a given year and the mean for the reference period (1999-2015) divided by the standard deviation of the reference period. The anomalies for sections were calculated using a general linear model using station, season, and year while the high frequency sampling stations only used season and year as inputs and were based on all available seasonal data. The NAFO Subareas are generally sorted by latitude from north (top) to south (bottom) regions. High frequency sampling stations are identified with an asterisk.

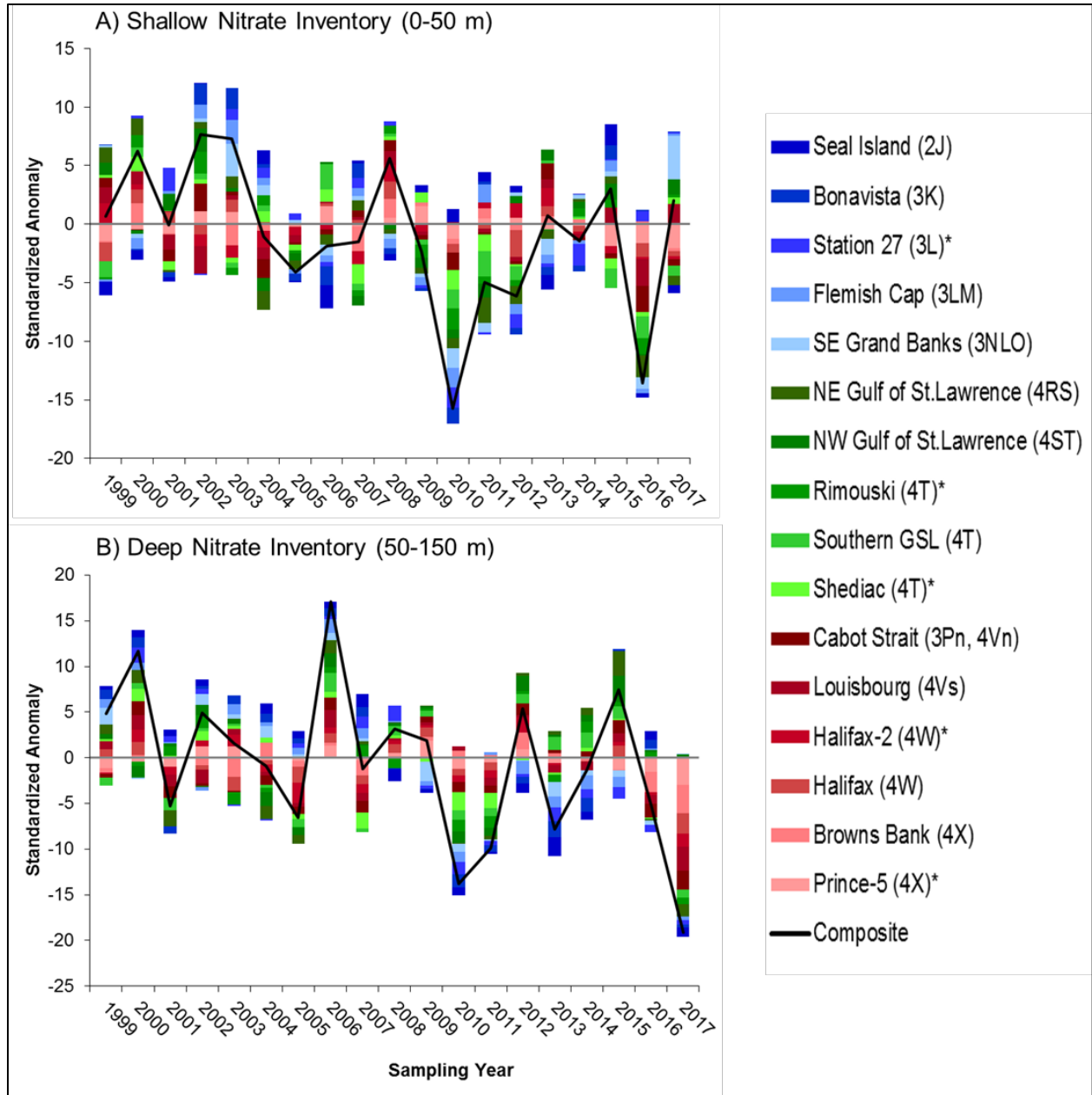


**Fig. 3** Time series of (A) shallow (0-50m) and (B) deep (50m-150m) nitrate (combined nitrite and nitrate) inventory anomalies from different oceanographic sections and high frequency sampling stations from the AZMP during 1999-2017. The anomalies for sections were calculated using a general linear model using station, season, and year while the fixed stations only used season and year as inputs and were based on all available seasonal data. The standardized anomalies are the differences between the annual mean for a given year and the mean for the reference period (1999-2015) divided by the standard deviation of the reference period. The contribution from each of the NAFO Subareas is represented by colour and height of the vertical bar. The solid black line is the cumulative (composite) anomaly across all Subareas in a given year. High frequency sampling stations are identified with an asterisk.

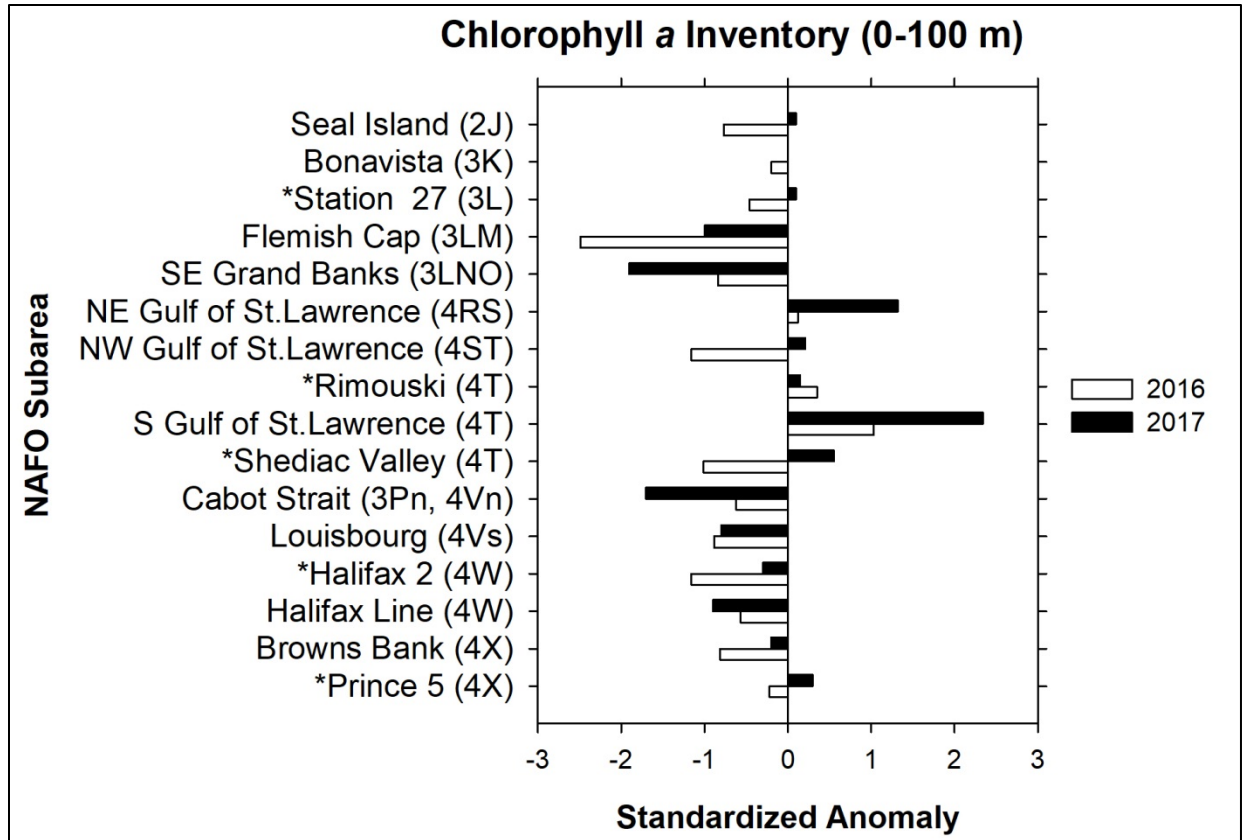


**Fig. 4** Summary of chlorophyll *a* inventory (0-100 m) from different oceanographic sections and high frequency sampling stations during the 2016 and 2017 AZMP surveys. The standardized anomalies are the differences between the annual mean for a given year and the mean for the reference period (1999-2015) divided by the standard deviation of the reference period. The chlorophyll *a* anomalies for sections were calculated using a general linear model using station, season, and year while the high frequency sampling stations only used season and year as inputs and were based on all available seasonal data. The NAFO Subareas are generally sorted by latitude from north (top) to south (bottom) regions. High frequency sampling stations are identified with an asterisk.

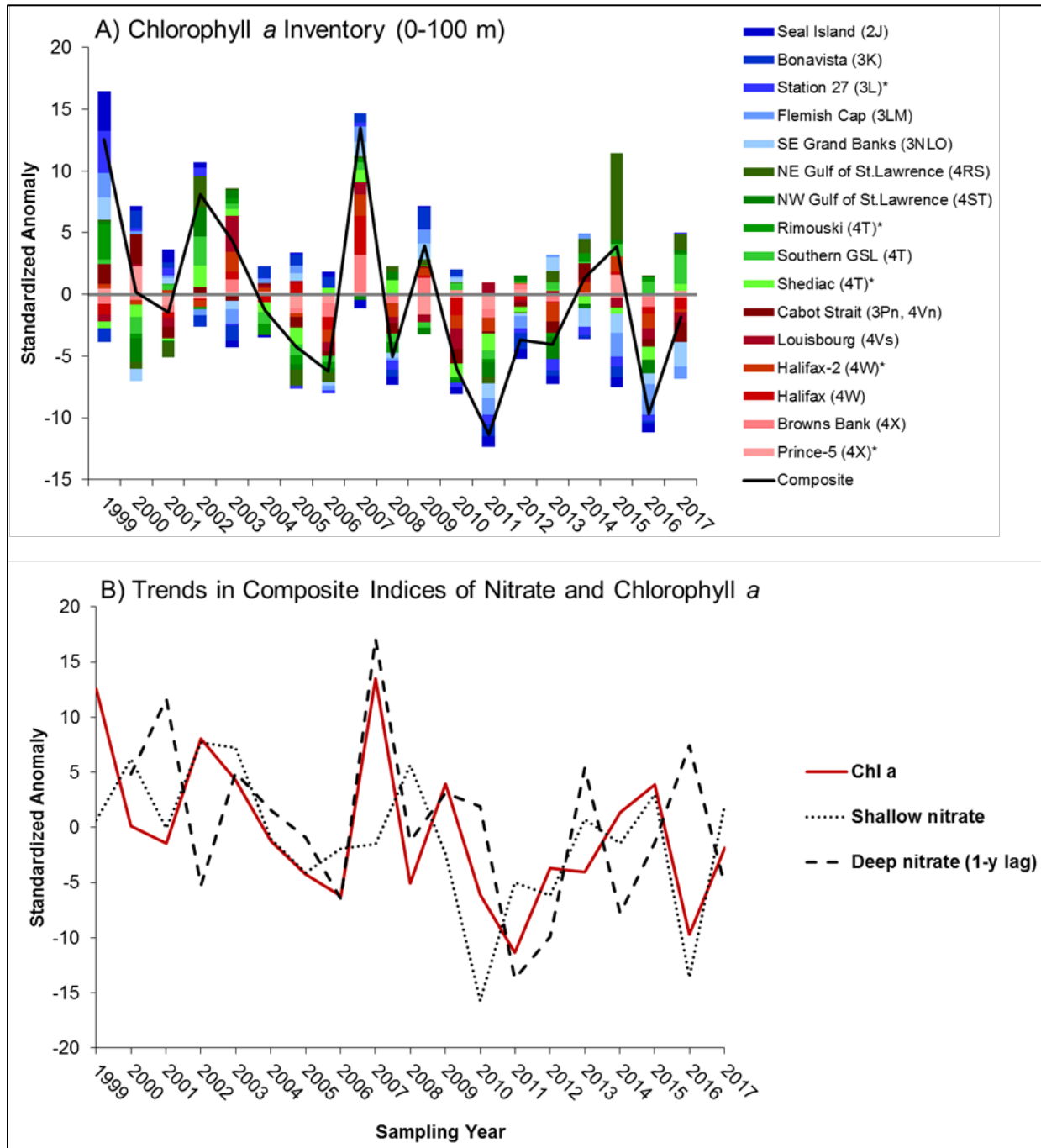


**Fig. 5** (A) Time series of chlorophyll *a* (0-100 m) inventory anomalies from different oceanographic sections and high frequency sampling stations from the AZMP during 1999-2017. The anomalies for each area were calculated using a general linear model using station, season, and year while the high frequency stations only used season and year as inputs and were based on all available seasonal data. The contribution from each of the NAFO Subareas to the cumulative anomaly of a given year is represented by colour and height of the vertical bar. The solid black line is the cumulative (composite) anomaly across all Subareas in a given year. (B) Comparison between composite anomaly time series of shallow nitrate (0-50m), deep nitrate (50-150m) and chlorophyll *a*.

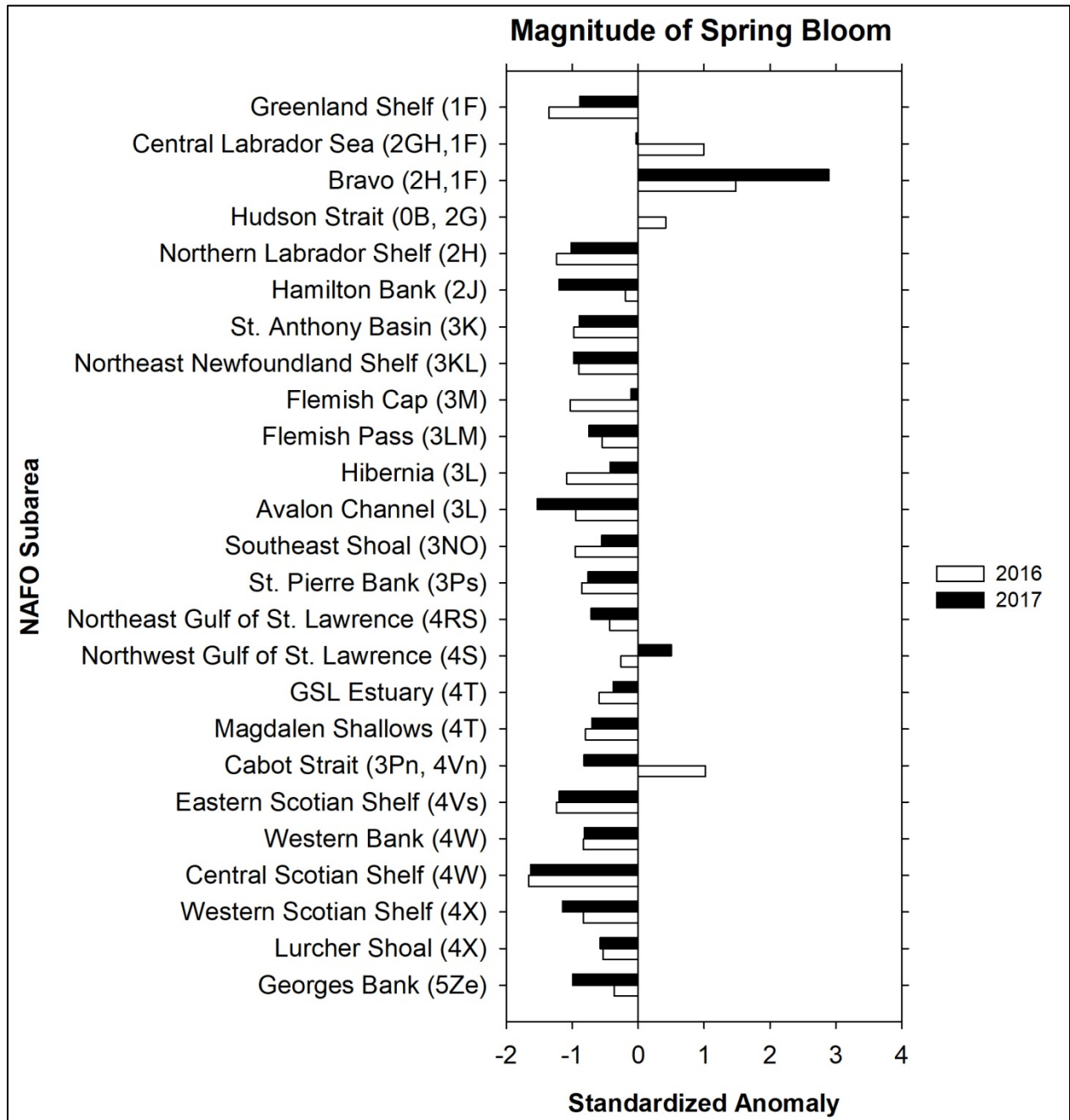


**Fig. 6** Summary of annual ocean colour anomalies for the total production (magnitude) of the spring bloom from VIIRS sensors across the different statistical subregions during 2015-2017. The standardized anomalies are the differences between the annual average for a given year and the long-term mean (1998-2015) divided by the standard deviation. The NAFO Subareas are sorted from northern (top) to southern (bottom) regions.

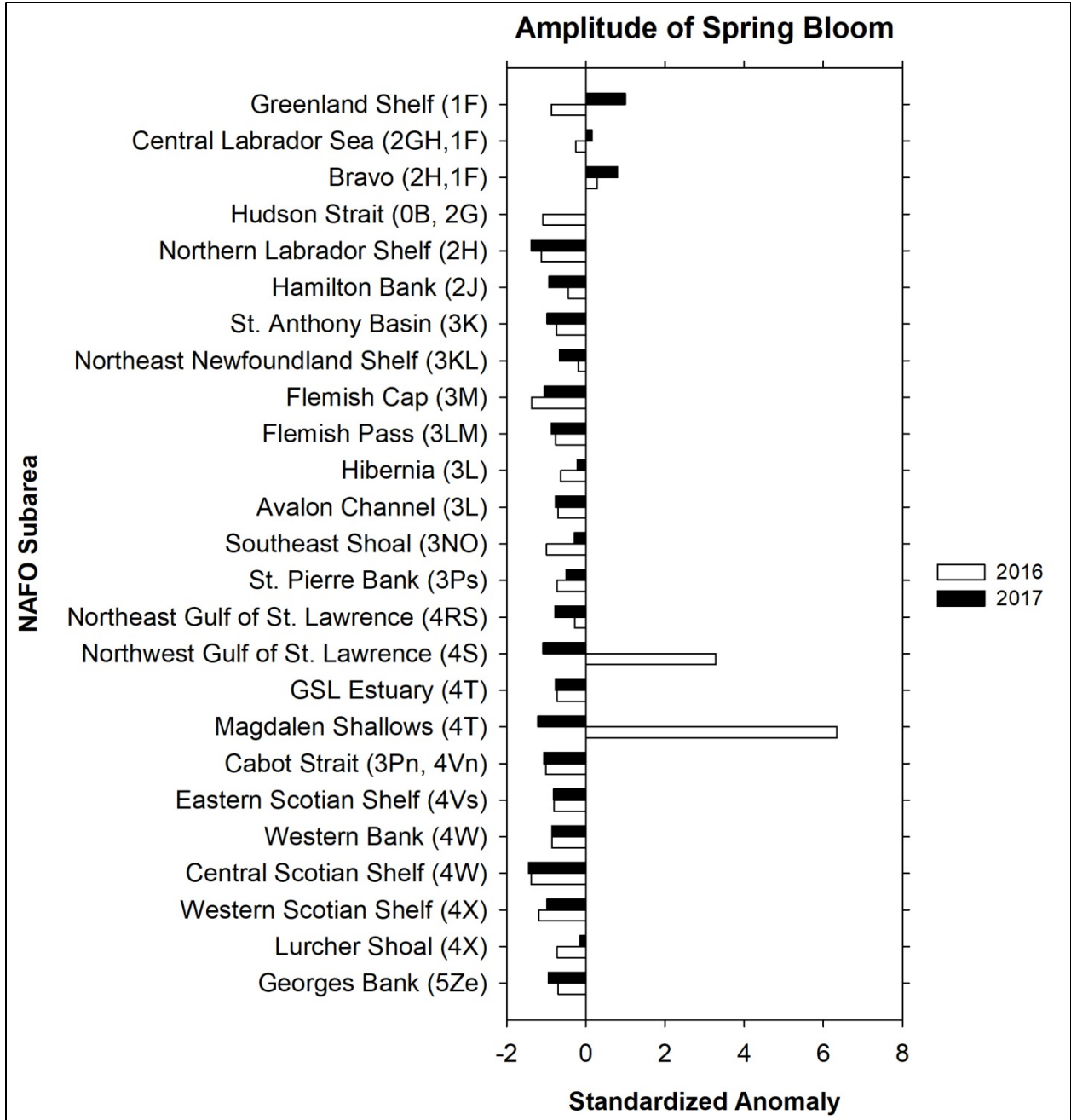


**Fig. 7** Summary of annual ocean colour anomalies for the maximum production (peak intensity) of the spring bloom from VIIRS sensors across the different statistical subregions during 2015-2017. The standardized anomalies are the differences between the annual average for a given year and the long-term mean (1998-2015) divided by the standard deviation. The NAFO Subareas are sorted from northern (top) to southern (bottom) regions.

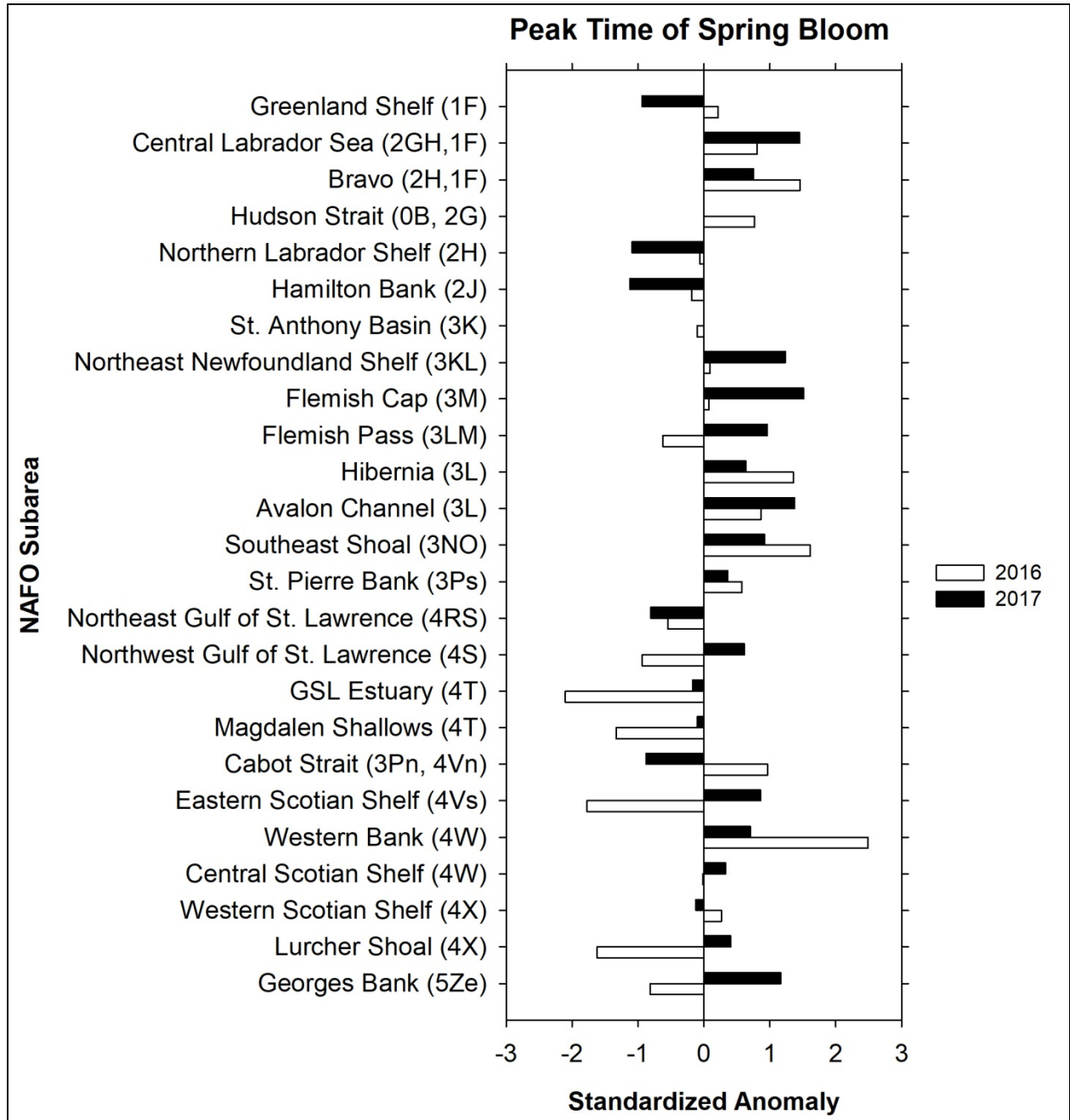


**Fig. 8** Summary of annual ocean colour anomalies for the time of maximum intensity (peak timing) of the spring bloom from VIIRS sensors across the different statistical subregions during 2015-2017. The standardized anomalies are the differences between the annual average for a given year and the long-term mean (1998-2015) divided by the standard deviation. The NAFO Subareas are sorted from northern (top) to southern (bottom) regions. Negative anomalies for the timing indices indicate earlier blooms while positive anomalies indicate the opposite.

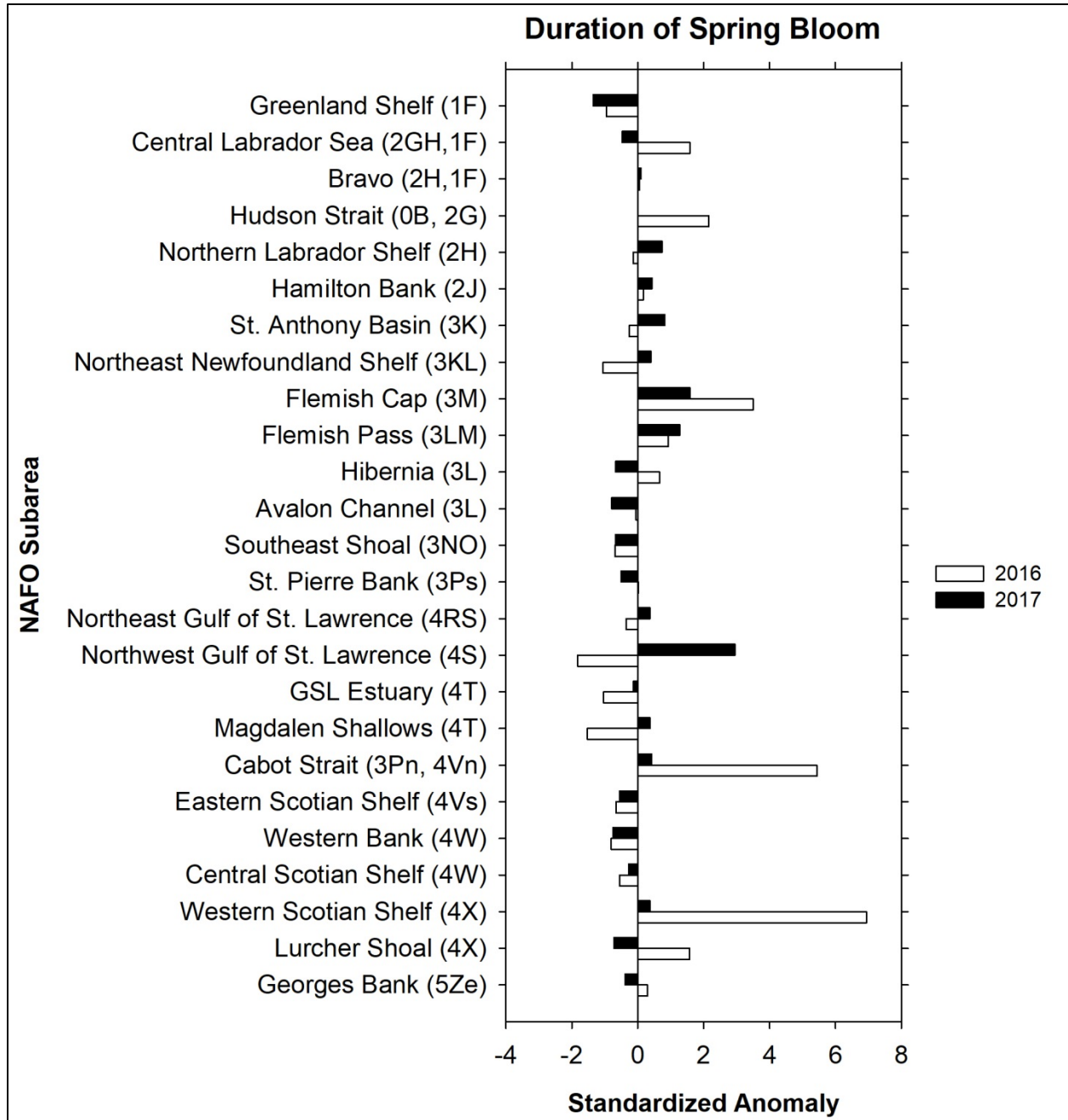


**Fig. 9** Summary of annual ocean colour anomalies for the duration of the spring bloom from VIIRS sensors across the different statistical subregions during 2016-2017. The standardized anomalies are the differences between the annual average for a given year and the long-term mean (1998-2015) divided by the standard deviation. The NAFO Subareas are sorted from northern (top) to southern (bottom) regions. Negative anomalies indicate shorter blooms while positive anomalies indicate the opposite.

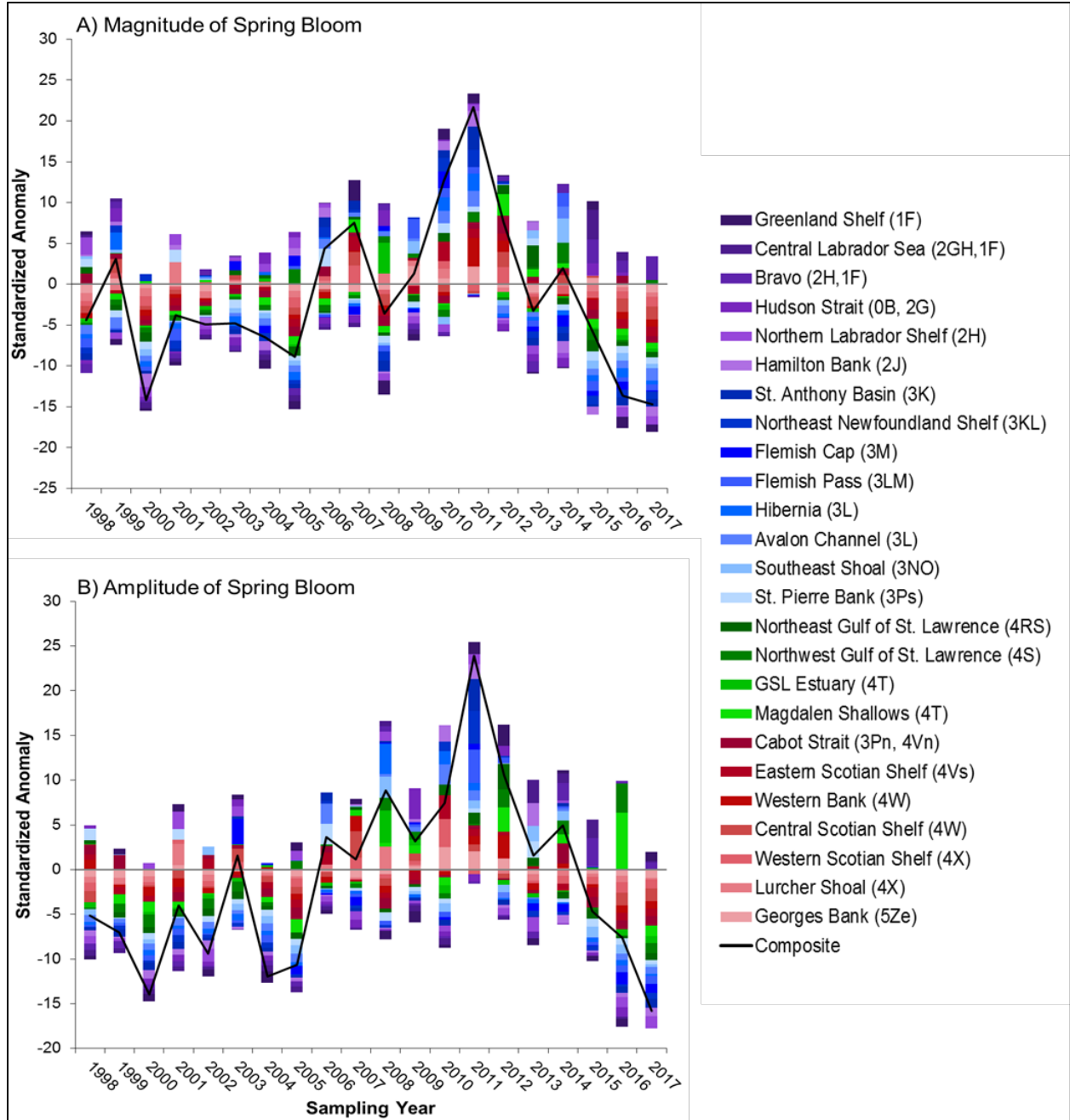


**Fig. 10** Annual anomaly time series for (A) the magnitude and (B) the amplitude of the spring bloom (integral of chlorophyll *a* concentration during the bloom in  $\text{mg m}^{-2} \text{d}^{-1}$ ) derived from weekly SeaWiFS, MODIS “Aqua”, and VIIRS sensor imagery across the different NAFO Subareas extending from Georges Bank to the Hudson Strait during 1998-2017. The standardized anomalies are the differences between the annual mean for a given year and the mean for the reference period (1999-2015) divided by the standard deviation of the reference period. The statistical subregions are sorted from northern (top) to southern (bottom) boxes. Data for Flemish Cap were not available during 1998-2002. The contribution from each of the NAFO Subareas is represented by colour and height of the vertical bar. The solid black line is the cumulative (composite) anomaly across all Subareas in a given year.



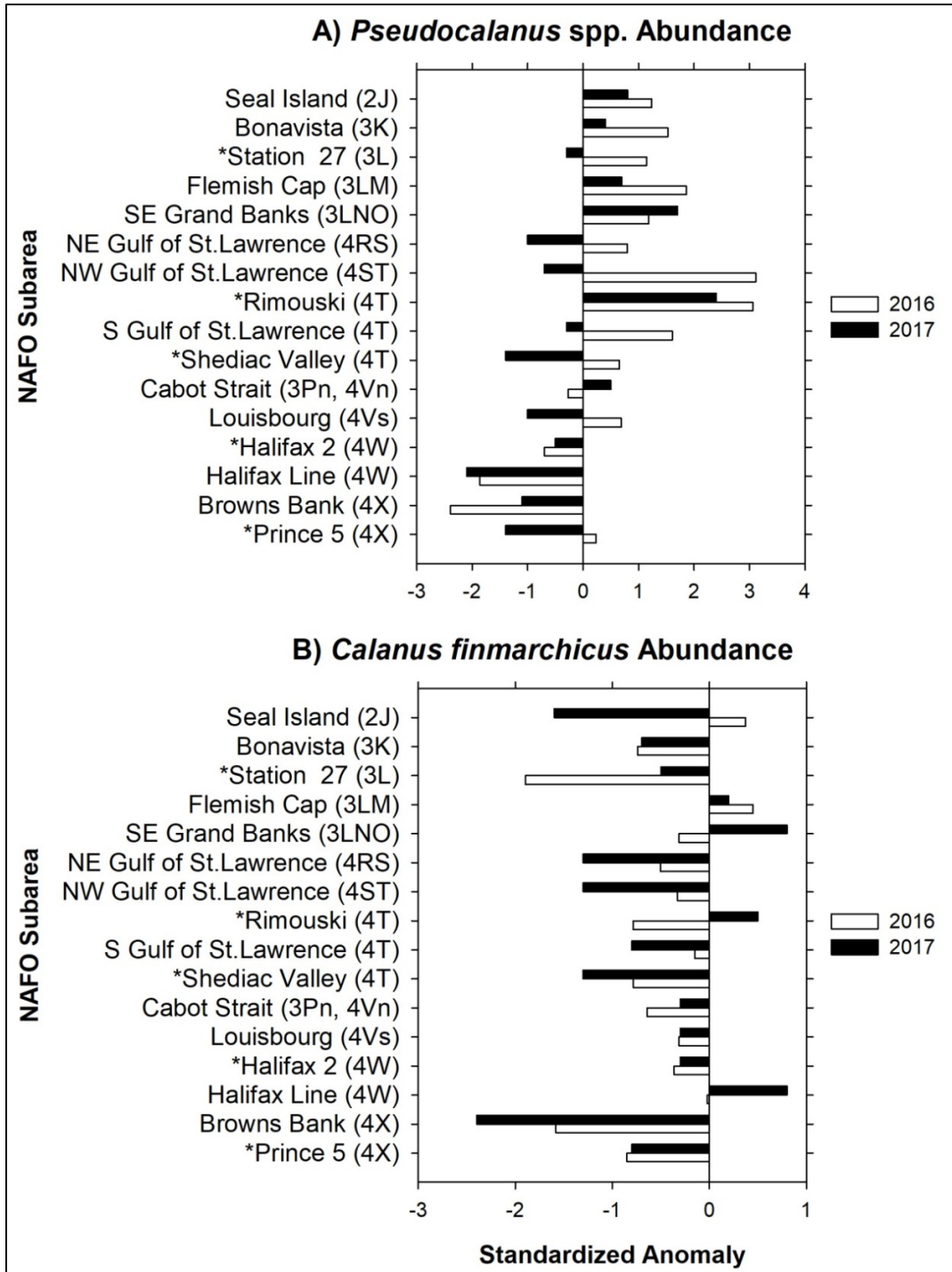


**Fig. 12** Summary of zooplankton abundance anomalies from different oceanographic sections and high frequency sampling stations from the Atlantic Zone Monitoring Program in 2017. *Pseudocalanus* spp. (top panel) and *Calanus finmarchicus* (bottom panel) represent dominant and ecologically important copepod taxa in the NW Atlantic. The zooplankton abundance anomalies for sections were calculated using a general linear model using station, season, and year while the high frequency sampling stations only used season and year as inputs and were based on all available seasonal data. The NAFO Subareas are generally sorted by latitude from the southern Labrador Shelf - 2J (top) to southern Scotian Shelf - 4X (bottom).

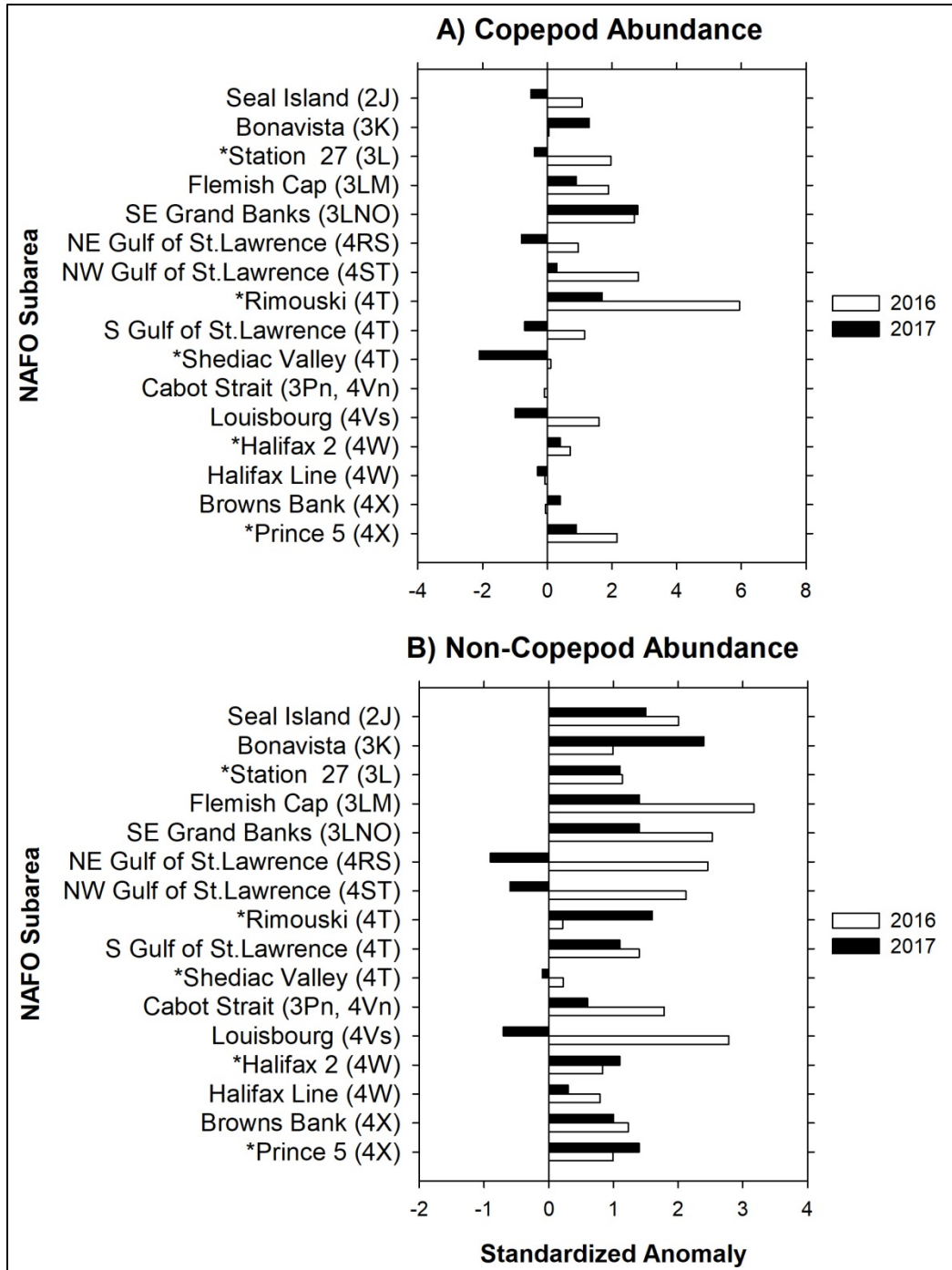


**Fig. 13** Summary of total copepods (top panel) and non-copepod (bottom panel) abundance anomalies from different oceanographic sections and high frequency sampling stations from the Atlantic Zone Monitoring Program during 2017. The zooplankton abundance anomalies for sections were calculated using a general linear model using station, season, and year while the high frequency sampling stations only used season and year as inputs and were based on all available seasonal data. The NAFO Subareas are sorted by latitude from the southern Labrador Shelf - 2J (top) to southern Scotian Shelf - 4X (bottom).

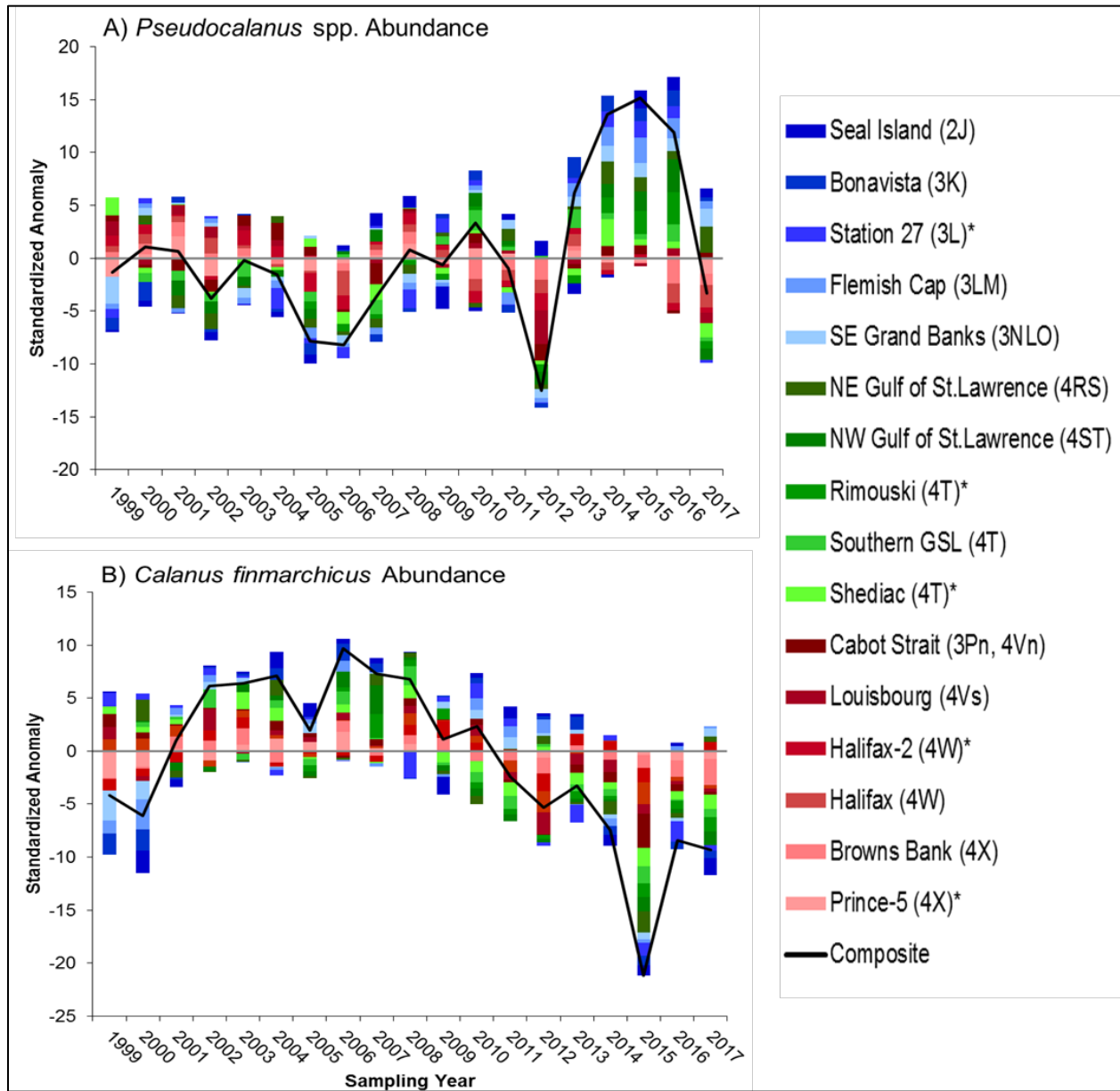


**Fig. 14** Time series of dominant copepods *Pseudocalanus* spp. (top panel), and *Calanus finmarchicus* (bottom panel) abundance anomalies from different oceanographic sections and high frequency sampling stations from the Atlantic Zone Monitoring Program during 1999-2017. The abundance anomalies for sections were calculated using a general linear model using station, season, and year while the high frequency sampling stations only used season and year as inputs and were based on all available seasonal data. The standardized anomalies are the differences annual and reference period (1999-2015) means divided by the standard deviation of the reference period. The contribution from each of the NAFO Subareas to the annual cumulative (composite) anomaly represented by the solid black bar is represented by colour and height of the vertical bar.

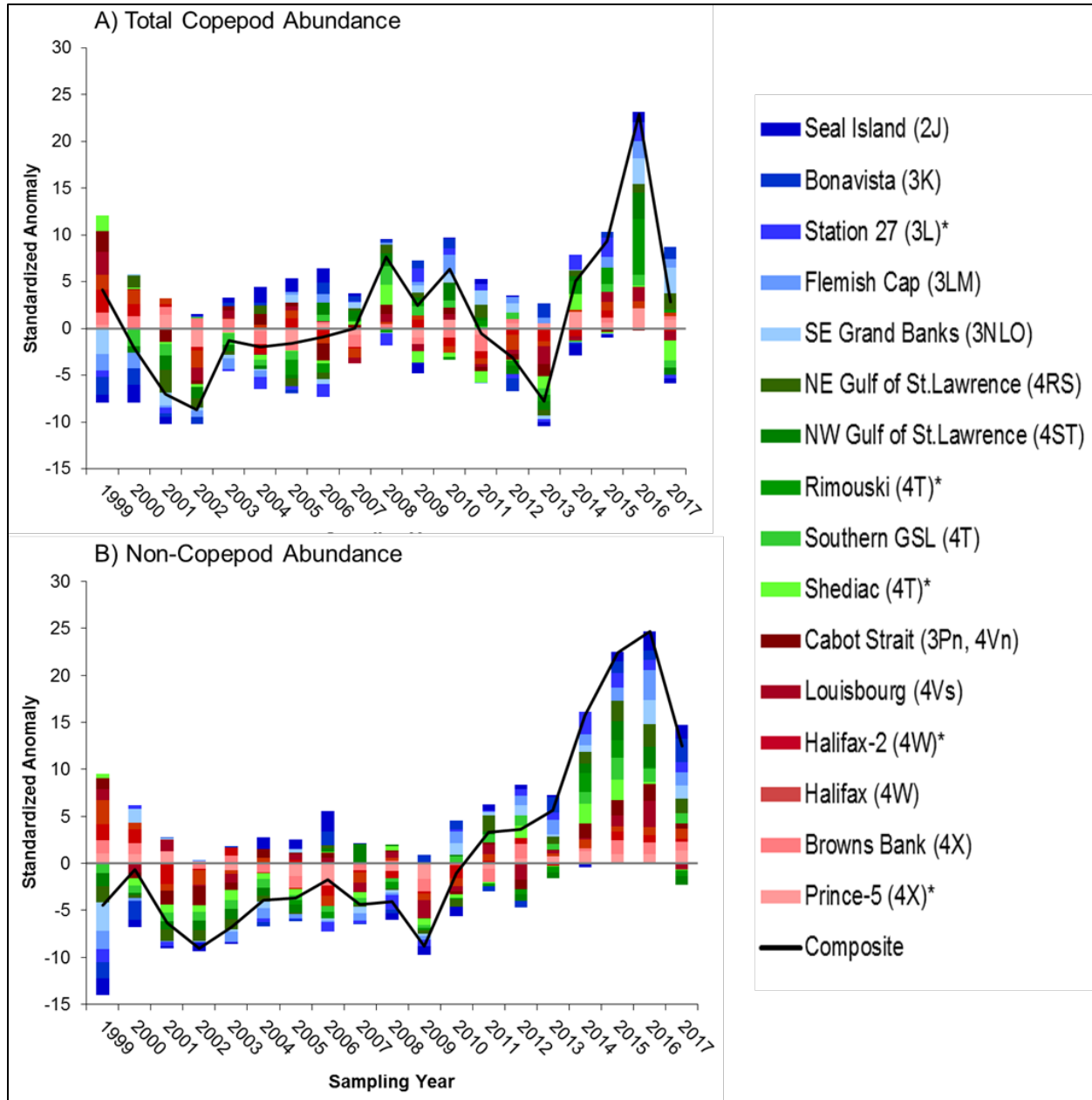


**Fig. 15** Time series of total copepod (top panel) and non-copepod (lower panel) abundance anomalies from different oceanographic sections and high frequency sampling stations from the Atlantic Zone Monitoring Program during 1999-2017. The zooplankton abundance anomalies for sections were calculated using a general linear model using station, season, and year while the high frequency sampling stations only used season and year as inputs and were based on all available seasonal data. The standardized anomalies are the differences between annual and reference period (1999-2015) means divided by the standard deviation of the reference period. The contribution from each of the NAFO Subareas to the annual cumulative (composite) anomaly represented by the solid black bar is represented by colour and height of the vertical bar.

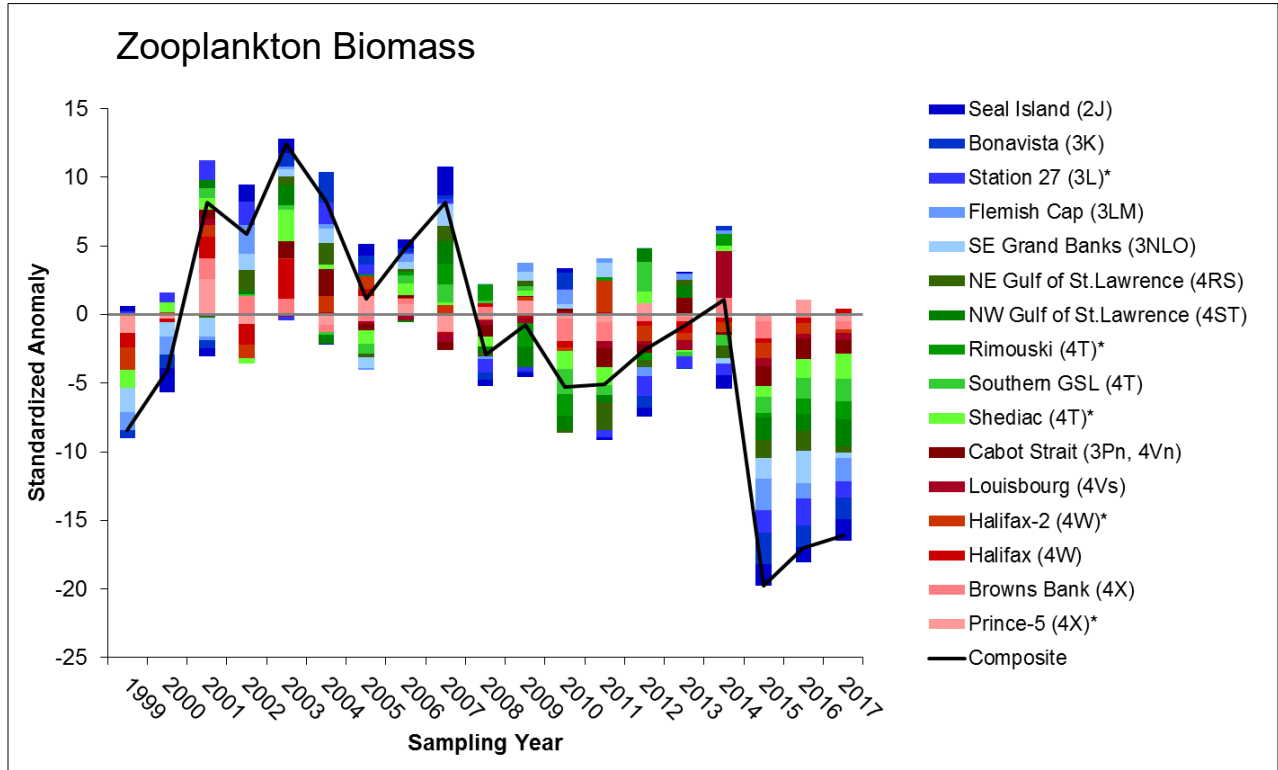


**Fig. 16** Time series of zooplankton (copepods and non-copepods) biomass anomalies from different oceanographic sections and high frequency sampling stations from the AZMP during 1999-2017. The anomalies for each area were calculated using a general linear model using station, season, and year while the high frequency stations only used season and year as inputs and were based on all available seasonal data. The contribution from each of the NAFO Subareas to the cumulative anomaly of a given year is represented by colour and height of the vertical bar. The solid black line is the cumulative (composite) anomaly across all Subareas in a given year.

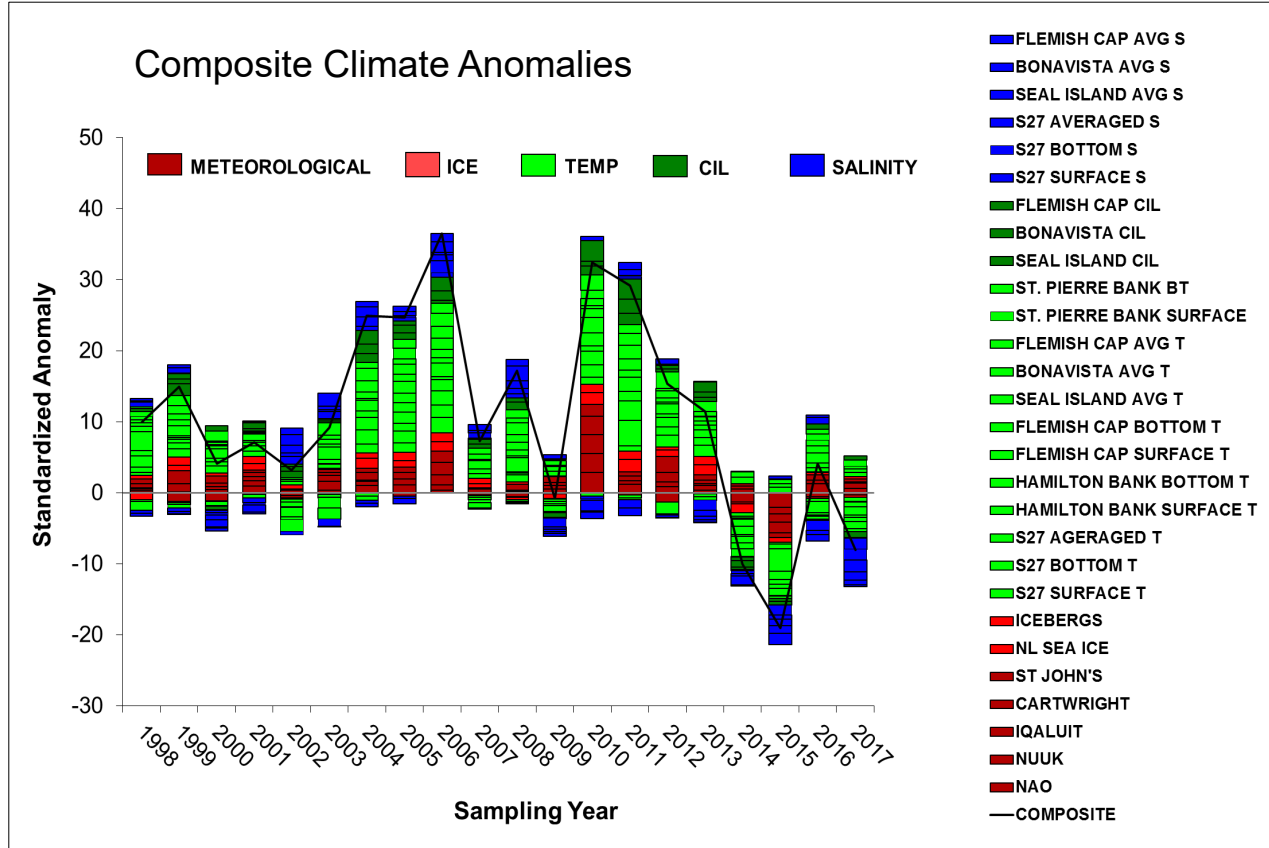


**Fig. 17** Time series of composite climate anomalies derived from physical environment indices (air temperature (meteorological), sea ice, surface temperature, bottom temperature, cold intermediate layer (CIL) temperature and salinity) collected at 28 sampling stations in the NW Atlantic from 1998-2017. The standardized anomalies are the differences between the annual mean for a given year and the mean for the reference period (1981-2010) divided by the standard deviation of the reference period. The contribution from each sampling station is represented by colour and height of the vertical bar. The solid black line is the cumulative (composite) anomaly across all sampling stations in a given year.

Anomaly Time Series	Shallow nitrate	Deep nitrate	Chl $a$	Magnitude	Amplitude	Duration	Peak Timing	<i>Pseudocalanus</i> spp.	<i>Calanus finmarchicus</i>	Total copepod	Non-copepod	Zooplankton biomass
Shallow nitrate												
Deep nitrate	0.98											
Chl $a$	0.03	0.09										
Magnitude	0.11	0.21	0.77									
Amplitude	0.22	0.14	0.16	0.00								
Duration	0.59	0.17	0.21	0.08	0.00							
Peak Timing	0.01	0.34	0.33	0.05	0.25	0.89						
<i>Pseudocalanus</i> spp.	0.76	0.47	0.88	0.40	0.86	0.78	0.02					
<i>Calanus finmarchicus</i>	0.73	0.45	0.81	0.34	0.51	0.74	0.18	0.01				
Total copepod	0.04	0.82	0.38	0.55	0.99	0.49	0.75	0.01	0.08			
Non-copepod	0.20	0.46	0.18	0.35	0.80	0.89	0.25	0.00	0.00	0.00		
zooplankton biomass	0.25	0.33	0.32	0.43	0.62	0.59	0.99	0.06	0.00	0.00	0.00	

**Fig. 18** Summary of relationships among zonal (NW Atlantic) composite anomaly time series. Anomalies for nitrate (shallow and deep), chlorophyll  $a$  (Chl  $a$ ), zooplankton abundance (*Pseudocalanus* spp., *Calanus finmarchicus*, total copepod and non-copepod) and zooplankton biomass are derived from AZMP surveys covering the period 1999-2017. Phytoplankton bloom anomalies (magnitude, amplitude, peak timing and duration) are derived from satellite ocean color data covering the period 1998-2017. Numbers ( $p$ -values) indicate the significance of Pearson correlation between two composite anomaly time series. Green squares indicate significant positive correlations; red squares indicate negative significant correlations.

Anomaly Time Series	Climate	Shallow nitrate	Deep nitrate	Chl <i>a</i>	Magnitude	Amplitude	Duration	Peak Timing	<i>Pseudocalanus</i> spp.	<i>Calanus finmarchicus</i>	Total copepod	Non-copepod	Zooplankton biomass
Climate													
Shallow nitrate	0.08												
Deep nitrate	0.30	0.53											
Chl <i>a</i>	0.00	0.14	0.48										
Magnitude	0.02	0.33	0.35	0.00									
Amplitude	0.00	0.00	0.35	0.03	0.23								
Duration	0.92	0.64	0.14	0.43	0.00	0.99							
Peak Timing	0.43	0.38	0.02	0.43	0.41	0.08	0.05						
<i>Pseudocalanus</i> spp.	0.00	0.98	0.00	0.16	0.42	0.01	0.47	0.01					
<i>Calanus finmarchicus</i>	0.00	0.99	0.89	0.00	0.08	0.33	0.66	0.61	0.39				
Total copepod	0.93	0.91	0.04	0.87	0.89	0.93	0.72	0.01	0.01	0.09			
Non-copepod	0.23	0.73	0.01	0.28	0.46	0.27	0.82	0.00	0.00	0.72	0.00		
zooplankton biomass	0.02	0.82	0.22	0.01	0.26	0.47	0.20	0.15	0.01	0.00	0.54	0.06	

**Fig. 19** Summary of relationships among regional (Newfoundland and Labrador) composite anomaly time series. Climate anomalies are derived from a set of meteorological; sea ice; water temperature and salinity indices. Anomalies for nitrate (shallow and deep), chlorophyll *a* (Chl *a*), zooplankton abundance (*Pseudocalanus* spp., *Calanus finmarchicus*, total copepod and non-copepod) and zooplankton biomass are derived from AZMP surveys covering the period 1999-2017. Phytoplankton bloom anomalies (magnitude, amplitude, peak timing and duration) are derived from satellite ocean color data covering the period 1998-2017. Numbers (*p*-values) indicate the significance of Pearson correlation between two composite anomaly time series. Green squares indicate significant positive correlations; red squares indicate negative significant correlations.